UNDERSTANDING CIRCADIAN CLOCK REGULATION OF RIBOSOME HETEROGENEITY IN NEUROSPORA CRASSA

A Thesis

by

AMANDA LEE PETTY

Submitted to the Office of Graduate and Professional Studies of
Texas A&M University
in partial fulfillment of the requirements for the degree of

MASTER OF SCIENCE

Chair of Committee,	Deborah Bell-Pedersen
Committee Members,	Matthew Sachs
	Junjie Zhang
Head of Department,	Thomas McKnight

August 2018

Major Subject: Microbiology

ABSTRACT

The circadian clock is a conserved mechanism that allows organisms to coordinate their daily physiology and behavior with 24-hour environmental cycles. The pervasiveness of the circadian clock is evident in that roughly half of mRNAs in eukaryotes accumulate with a circadian rhythm. The fungus, *Neurospora crassa*, has served as a model system to understand how the circadian clock influences daily rhythms and gene expression. In addition to transcriptional control of the circadian clock, there is evidence to support clock regulation of post-transcriptional, translational, and post-translational control of gene expression. Previous studies in the Bell-Pedersen lab demonstrated that the clock regulates the stress-associated p38 MAPK pathway, which in turn, regulates the activity of translation elongation factor eEF2 in *N. crassa*. In addition, our lab has discovered that the activity of eukaryotic initiation factor 2α (eIF2α) is clock-controlled. Moreover, recent preliminary data from mass spectrometry suggested that the clock controls the amount of ribosomal proteins associated with ribosomes, which in turn may lead to rhythms in mRNA translation. This mass spectrometry data identified 15 ribosomal proteins and their variants as candidates to examine for rhythmicity. In this study, I test the idea that the composition of the ribosome changes throughout the day. First, I generated homokaryons of V5-tagged ribosomal proteins, RPL27 and RPS19, indicating that the tagged proteins maintain some level of function. Next, I showed that RPL27-V5 and RPS19-V5 abundance in pelleted ribosomes was not rhythmic. Finally, I discovered that the cellular ratio of ribosomal components showed no obvious time of day difference in two timepoints (DD12 and DD24). Similar analyses of ribosomal component ratios in RPL25-FLAG and RPL27-V5; RPL25-FLAG strains suggested that these epitope tags may partially interfere with ribosome activity. Despite these challenges,

there are thirteen additional ribosomal proteins remaining to be independently validated for rhythmicity, and while this method shows promise, caution must be taken when using tags on the ribosomal proteins. Therefore, futures studies will be performed with an alternative tagging method or using ribosomal protein antibodies to monitor rhythms in the endogenous ribosomal proteins.

ACKNOWLEDGEMENTS

I would like to gratefully acknowledge the guidance, support, encouragement and constant motivation of my mentor and committee chair, Dr. Deborah Bell-Pedersen. Under her guidance I obtained many invaluable skills, both personally and professionally, and for that I am grateful. I am also thankful for my committee members, Dr. Matthew Sachs and Dr. Junjie Zhang for their guidance and support throughout the course of this research.

Many thanks also go to my friends and colleagues and the department faculty and staff for making my time at Texas A&M University a great experience. I would also like to extend my gratitude to all my colleagues in the lab: Dr. Teresa Lamb, Dr. Kathrina Castillo, Oneida Ibarra, Shanta Karki, Jennifer Jung, Zhoalan Ding, and Johnny Fazzino.

Finally, I would like to thank my parents, Ralph and Katha Petty, for constantly supporting me and helping me strive to be the best possible person I can be. Without their constant guidance and understanding, graduate school would not have been possible. I would also like to thank my sister, Maddie Petty, for always keeping a smile on my face and being one of my best friends. I would also like to acknowledge all my grandparents for always being some of my biggest cheerleaders.

CONTRIBUTORS AND FUNDING SOURCES

This work was supported by a thesis committee consisting of Professor Deborah Bell-Pedersen and Matthew Sachs of the Department of Biology and Professor Junjie Zhang of the Department of Biochemistry and Biophysics.

MS/MS data was conducted by Drs. William Russell and Dave Russell in the Laboratory for Biological Mass Spectrometry in the Department of Chemistry at Texas A&M University, and Samuel Purvine and Erica Zink at the Environmental Molecular Scientific Laboratories (EMSL) in Richland, WA. The MS/MS data was analyzed for rhythmicity by Dr. Kathrina Castillo in the Bell-Pedersen lab, Department of Biology at Texas A&M University.

The FLAG tagged strain of RPL25 (DBP2512) was made by graduate student Lunda Chen in Dr. Matthew Sachs lab in the Department of Biology at Texas A&M University.

The polysome profiles were conducted with Dr. Cheng Wu, a postdoctoral fellow in Dr. Matthew Sachs and Dr. Bell-Pedersen's labs, and Dr. Teresa Lamb in the Bell-Pedersen lab, Department of Biology at Texas A&M University.

All other work conducted for the dissertation was completed by the student independently.

Graduate study was supported by a grant from the National Institutes of Health, GM058529 to Dr. Bell-Pedersen. Mass spectrometry conducted at EMSL was supported by a grant from the JGI-EMSL Collaborative Science Initiative (JECSI) to Dr. Bell-Pedersen.

TABLE OF CONTENTS

LIST OF FIGURES

Page

LIST OF TABLES

Page

1. INTRODUCTION

1.1 The circadian clock

The circadian clock is an endogenous biological mechanism which enables an organism to anticipate and adapt to 24-hour environmental cycles [16, 32, 45]. There are three main criteria all circadian clocks must meet [1, 3]: First, in constant conditions, such as constant darkness (DD), the endogenous free-running clock must have a period of around 24 hours. Second, the clock must be entrainable, meaning it can be reset by an environmental signal. Third, the clock must be temperature-compensated, meaning the rhythm is relatively constant over biologically relevant temperatures. Circadian clock systems are present in prokaryotes and eukaryotes, ranging from cyanobacteria to humans [3, 29, 32]. In higher eukaryotes with differentiated tissues, the clock coordinates the timing of physiology and behavior among the tissues and cell types [16, 32, 45]. The clock is highly important to human health, as its disruption can increase the risk of certain forms of cancer, heart disease, type-2 diabetes, as well as lead to psychological problems such as depression, mania, and schizophrenia [21, 28, 43, 58].

Because the circadian clock is critical to human health and to the life cycle of other eukaryotes, it is important to understand how the clock regulates rhythmic gene expression. While great advances have been made in our understanding of how the clock controls transcription, much is still unknown about how the circadian clock regulates gene expression post-transcriptionally, including mRNA translation. Therefore, the aim of this study is to examine if the circadian clock regulates the composition of ribosomes through examining time-of-day associations of specific ribosomal proteins with the ribosome.

1.2 Circadian clock components

The circadian clock system contains three main components: 1) input pathways, which entrain the clock to the 24-hour environmental cycle, 2) one or more oscillators, which drive conserved molecular time keeping mechanisms that free run with a period of close to 24 hours in constant conditions, and 3) output pathways which pass the time-of-day information from the core oscillator to regulate gene expression and overt rhythmicity [1, 38, 59]. The core circadian oscillator is well conserved throughout all eukaryotes and contains an interconnected network of both positive and negative regulatory elements that form an autoregulatory negative feedback loop [16, 32, 45]. In a typical circadian autoregulatory loop, the positive elements activate expression of the negative elements. Over the course of the day, mRNA levels of the negative elements increase and are translated, leading to a subsequent increase in the protein levels. These negative elements feedback to inhibit the activity of the positive elements. Over time, there is degradation of negative components which releases inhibition of the positive elements allowing for a new cycle to start. This feedback is necessary for the circadian clock to free-run with a ~24-hour cycle in constant conditions.

1.3 Model organism *Neurospora crassa*

Neurospora crassa, a fungus in the phylum *Ascomycota*, is a filamentous haploid organism. *N. crassa* has been a model eukaryotic organism for both genetic [2] and circadian [17, 48] biology due to ease of growth, genetic tractability, and daily rhythmic behavior driven by a circadian oscillator. The circadian clock regulates many different aspects *N. crassa* biology, including conidiation [3], hyphal branching [16], and importantly gene expression [1, 22, 38, 59]. The *N. crassa* life cycle contains both a sexual cycle, which produces ascospores [5], and an asexual

cycle, which produces conidia, providing an advantage for genetic studies. During the asexual life cycle, macroconidia, conidia which contain more than one nuclei, are formed from aerial hyphae, which germinate under the appropriate conditions and produce mycelium [13]. These multinucleated macroconidia can either be homokaryotic, where there is only one genotype in all nuclei, or they can be heterokaryotic, whereby two or more nuclei contain differences in their genotype [13]. Heterokaryons allow maintenance of mutations in essential genes [13]. These organisms will contain nuclei with a WT genotype to ensure life, and nuclei which contain the mutant genotype of interest. Homokaryons of non-essential gene deletions are produced using the sexual life cycle where parent strains of different mating type fuse and undergo meiosis to produce eight haploid ascospores within an ascus [13]. Each ascospore contains only one nucleus, and are therefore homokaryotic.

1.4 *N. crassa* circadian clock

Because the core circadian clock mechanism is well conserved throughout all eukaryotes, our lab takes advantage of the genetic tractability of the filamentous fungus *N. crassa* to study how the circadian clock regulates rhythmic gene expression [1, 38]. In *N. crassa*, the circadian clock is composed of a core oscillator with positive and negative elements. The positive element of the clock is the White Collar Complex (WCC), which is composed of the blue light photoreceptor, WHITE COLLAR-1 (WC-1) and WHITE COLLAR-2 (WC-2). The negative arm of the clock contains FREQUENCY (FRQ) and FRQ-interacting RNA helicase (FRH) (Figure 1). In the subjective morning, the WCC binds to the *frq* promoter to promote transcription [19, 35]. Transcription of *frq* causes mRNA levels to increase during the daytime, and mRNA translation leads to an increase in FRQ protein throughout the day. FRQ then homodimerizes and interacts

with FRH to form the FRQ/FRH complex (FCC) [9, 10]. The FCC promotes phosphorylation and inactivation of the WCC, which in turn leads to inhibition of *frq* transcription [9, 10, 54]. Over the course of the day, FRQ is phosphorylated by multiple kinases and is subsequently degraded by the proteasome, causing decreased inhibition of the WCC [39]. Once FRQ is degraded, the WCC is then dephosphorylated allowing for the rhythmic cycle to restart the next day [19, 22, 54]. In constant dark conditions (DD), the circadian cycle is 22.5 hours long [44]. In nature, environmental cues, such as light and temperature, synchronize the cells to a 24 hour circadian cycle which matches the 24 day [8].

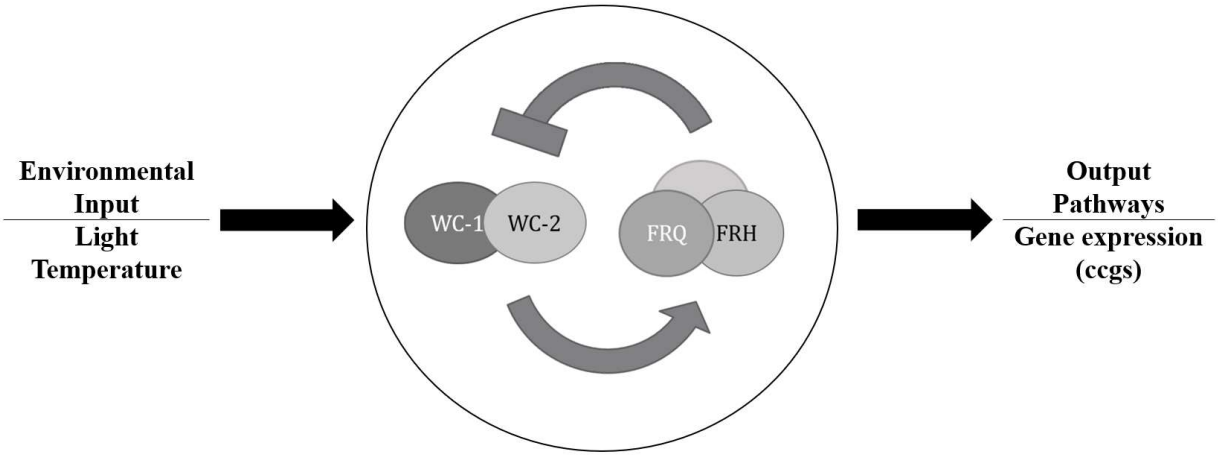

Figure 1. The *N. crassa* circadian clock system. See the text for detail describing the figure.

1.5 Post-transcriptional and translational regulation of the clock

The circadian clock is responsible for driving rhythms in accumulation of about 40% of the eukaryotic transcriptome [22, 30, 42, 46, 59]. One particularly interesting outcome of rhythmic gene expression is that it provides a mechanism to partition energy to metabolism. For example, in *N. crassa*, genes that are needed for catabolism peak primarily during the day, whereas genes needed for anabolism primarily peak at night [6, 22]. Many rhythmic mRNAs encode for ribosomal proteins or translation factors, suggesting that transcription rhythms could lead to rhythms in translation via rhythmic control of the translational machinery [27]. In addition to studies of circadian regulation of rhythmic transcription and mRNA, recent research has revealed that the clock can regulate gene expression at multiple post-transcriptional levels (S. Karki, unpublished) [7, 25, 26, 31, 36, 37]. Quantitative proteomic studies of the mouse liver have revealed that up to 50% of rhythmically accumulating soluble proteins are expressed from non-cycling mRNAs [22, 51], suggesting that the clock regulates protein synthesis or turnover. Our lab demonstrated that the clock controls translation initiation through rhythmic regulation of the activity of the translation initiation factor, eIF2α (S. Karki, unpublished), and elongation by circadian regulation of the activity of the translation elongation factor eEF2 [7]. Finally, several studies have suggested that the composition and activity of ribosomes can be regulated by environmental or developmental signals [18, 50, 53, 62], suggesting the possibility that the clock could also play a role in ribosome composition and function.

1.6 Evidence for regulation of ribosome components

Ribosome heterogeneity refers to the idea that individual ribosomes are not all identical translation machines. Ribosome heterogeneity may be the result of differences in association of

ribosomes with accessory proteins, ribosome protein modifications, or differential composition of ribosomal proteins within 80S ribosomes [22, 33, 49, 55, 60, 62]. Several pieces of data support the existence of ribosome heterogeneity. For example, in *Dictyostelium* there are differing levels of ribosomal proteins during different stages of development, allowing for some ribosome proteins to be more highly expressed in the fruiting body compared to the spore stage, or vice versa [49, 50, 62]. Through two-dimensional gel electrophoresis, it was discovered in the fruiting body stage of *Dictyostelium* that the ribosomal protein RPL18 is highly expressed, while in the amoeba stage RPL18 is expressed at much lower levels, suggesting that development may affect ribosome composition [50, 62]. In addition, in *Dictyostelium* there are developmental-stage-dependent post-translational modifications (phosphorylation and methylation) of ribosomal proteins that are necessary for translation of stage-specific mRNAs [49, 50]. In *Drosophila*, translational control can be mediated by the accessory protein, "Reaper," which is involved in apoptosis of cells during embryonic development and metamorphosis [60]. Reaper associates with the small ribosomal subunit and disrupts the cap scanning mechanism of translation initiation [11, 62] thereby facilitating the translation of specific mRNAs which increase apoptosis [11]. In developing mouse embryos, the somite and neural tube have increased gene expression in *rpl38*, and when *rpl38* is deleted, it results in a tail-short phenotype [33]. Additionally, it has been shown in the mammalian ribosome there are ribosome-associated proteins that allow the ribosome to be modified and translate specific mRNAs [56]. Importantly, several genome-wide circadian studies revealed rhythms in the accumulation of mRNAs encoding ribosomal proteins [12, 22, 55]. The levels of core ribosomal proteins in translating ribosomes were found to be heterogeneous in mouse embryonic stem cells, and these heterogenous ribosomes seem to preferentially translate subpools of mRNA [55]. Taken

together, these data support the hypothesis that the circadian clock may regulate mRNA translation, in part, through temporal regulation of ribosome heterogeneity.

1.7 Circadian clock control of ribosomal protein heterogeneity

To determine if the circadian clock regulates ribosomal protein levels, germinated conidia time courses of WT and ΔFRQ cells were performed [7]. Samples were cryogenically ground and pelleted using sucrose density centrifugation to enrich for ribosomes [40, 52]. The enriched ribosome samples were subjected to mass spectroscopy (MS/MS) at Texas A&M University (TAMU, 3 replicates) and the Environmental Molecular Scientific Laboratories (EMSL, Richland, WA, 3 replicates). The average peptide reads for the replicates were mapped to the *N. crassa* genome, and quantitated following normalization to a known concentration of enolase that was spiked into the samples (TAMU) or as previously described (EMSL) [47, 63]. Rhythmicity from each replicate was determined using MetaCycle [61]. Twelve cytoplasmic ribosomal proteins and three ribosomal protein variants cycled in abundance ($p \leq 0.05$), in WT cells, but not in ΔFRQ cells (Table 1). These ribosomal proteins were shown to peak in abundance at different times throughout the circadian cycle (Figure 2). Four out of the fifteen ribosomal proteins were predicted to be rhythmic in both data sets (Table 1). Importantly, the total cell weight (Figure 3), and most ribosomal proteins (e.g. RPL25, Figure 4), do not cycle. Dr. Kathrina Castillo in the Bell-Pedersen lab, discovered that the levels of RPL25-FLAG are arrhythmic in rhythmic *N. crassa* germinated conidia time course cultures (Figure 4), and present in constitutive amounts in enriched ribosomes at all times of day as evidence by MS/MS (Figure 2). Therefore, RPL25-FLAG provides an important control for validations of candidate rhythmic ribosomal proteins using dual-tagged ribosomes (e.g. RPL25-FLAG and rhythmic RP-V5).

Taken together, these data suggested that the levels of some ribosomal proteins associated with the 80S ribosome are controlled by the circadian clock, and support our idea that the clock regulates ribosome heterogeneity.

Ribosomal Protein	NCU	Rhythm TAMU	Rhythm EMSL	Peak Time
RPS11	03102		X	DD36
RPS19	07826	X	X	DD24
RPS6	08502	X	X	DD24
RPS8	08500		X	DD44
RPS9	01949		X	DD24/48
RPS9-V*	03827	X		DD36
RPL10 P0	07408	X		DD24
RPL19	05804	X		DD16
RPL19-V*	04614	X		DD24
RPL27	01827	X	X	DD24
RPL3	06843	X		DD24
RPL3-V*	08299	X		DD24
RPL35	10498	X		DD20
RPL39	08990		X	DD24
RPL8	04779	X	X	DD20

Table 1. Candidate rhythmic ribosomal proteins identified by MS/MS from either TAMU or EMSL. Predicted rhythmicity is marked by an X. Peak time is showed as hours in constant darkness, DD. Variants are marked with V*.

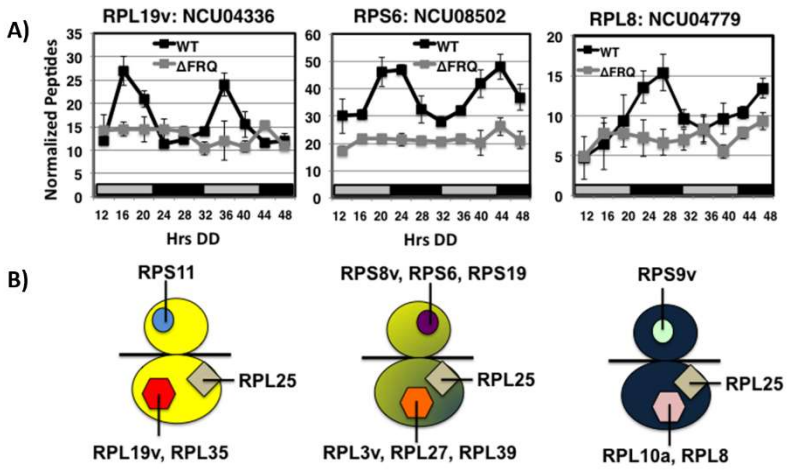

Figure 2. Circadian ribosome heterogeneity. Representative MS/MS on samples enriched for ribosomes from WT or ΔFRQ cells harvested in the dark (Hrs DD) every four hours and plotted as normalized peptide reads. A) Examples of r-proteins that peak at different times of the day in WT, but not in ΔFRQ cells, are shown. B) Cartoons summarize the r-proteins that were rhythmic in ribosomes and which peaked in the day (yellow), dusk (yellow/blue), or night (blue). v=variant. RPL25 is present in equal amounts in ribosomes at all times of the day. Values are mean ± SEM, n=3.

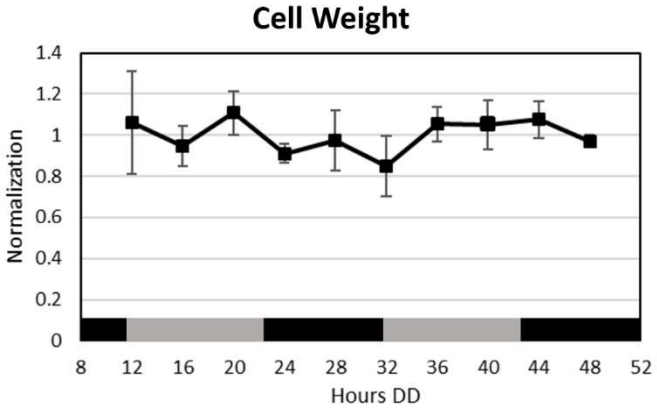

Figure 3. Total cell weight of rhythmic germinated conidia cultures are arrhythmic. Graph displays germinated conidia time course from cells normalized to 1. Values are mean ± SEM, n=3.

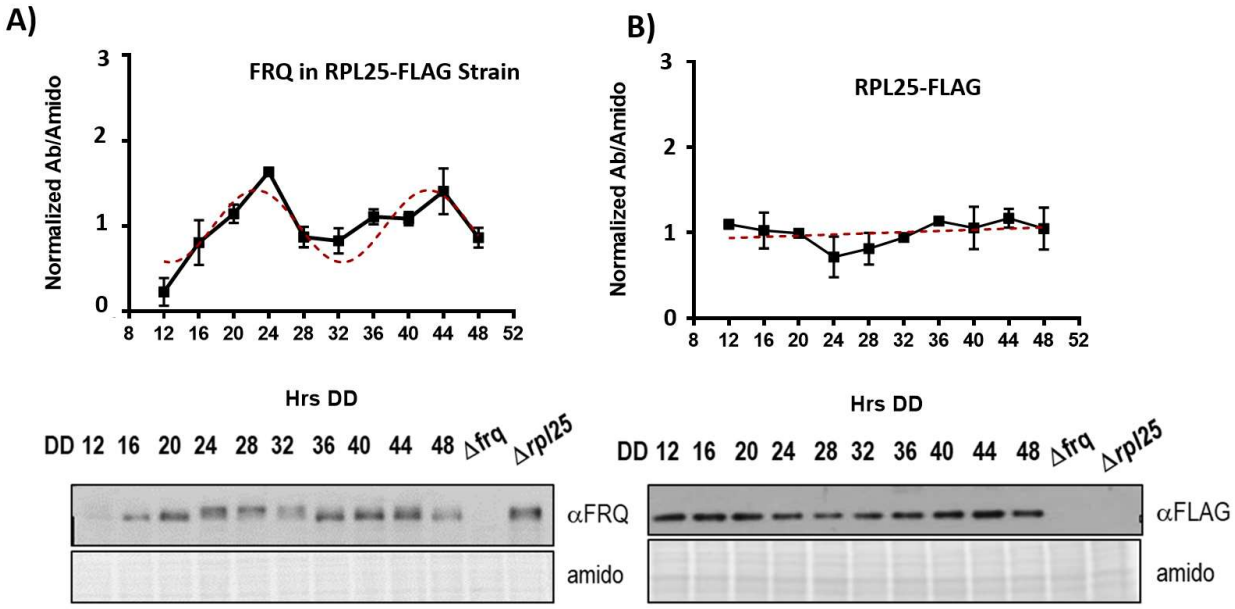

Figure 4. RPL25-FLAG protein levels from germinated conidia time courses are not rhythmic. Plot of FRQ (A), and RPL25-FLAG (B) protein levels (solid black line) determined by western blot (representative blots shown below) from samples harvested every 4 hours in DD. The average signal was normalized to amido black stained membrane protein loading. Control *Δfrq* and *Δrpl25* extracts are shown. Values in the plots are mean ± SEM, n=3. Rhythmicity was determined by F-test of fits to a sign wave (A) or a line (B) and are shown as a red-dotted line in the plots ($p \leq 0.05$).

1.8 Understanding circadian clock regulation of ribosome heterogeneity in *N. crassa*

To understand how the circadian clock regulates the composition of ribosomes in *N. crassa*, I focused on two ribosomal proteins, RPL27 and RPS19, identified as rhythmically associated with ribosomes in both TAMU and EMSL MS/MS data sets. I generated V5-epitope-tagged homokaryons of RPL27 and RPS19 to examine their protein levels in pelleted ribosomes. I examined sucrose density gradient profiles of a WT strain to determine if there was an obvious time-of-day difference in the ratio of the translational machinery components. Additionally, I

examined if the epitope tags in the RPL25-FLAG and dual tagged RPL27-V5; RPL25-FLAG strain affect the sucrose density gradient profiles of ribosomal components. One long-term goal was to develop a method to identify ribosomal proteins that are rhythmically associated with translating ribosomes, and use these heterogenous ribosomes to determine what effect they have on translation.

2. MATERIALS AND METHODS

2.1 Strains and culture maintenance

Neurospora crassa wild-type strain, 74-OR23 (FGSC 2489, WT), was obtained from the Fungal Genetics Stock Center (FGSC, Kansas State University, Manhattan, KS, http://www.fgsc.net). RPL25-FLAG (DBP2512) was obtained from Lunda Chen in Dr. Mathew Sachs lab. RPL25-FLAG contains a deletion of the endogenous *rpl25 (*NCU06226*)* gene and a copy of RPL25 tagged at the C-terminus with FLAG and 6xHIS and inserted at the *his-3* locus (Δ*rpl25::hph*, *his3*$^{+}$::*rpl*25::FLAG-His6x). WT strains were grown on Vogel's minimal medium (VM: 1x Vogel's and 2% glucose). Strains resistant to hygromycin-B were grown on VM containing 200 µg/mL of hygromycin B, *Streptomyces sp*. (Calbiochem, Darmstadt, Germany). All strains used in this study are listed in Table 2.

Symbol	DBP	NCU/FGSC	Genotype
WT	DBP984	FGSC 2489	*Wild-type* 74-OR23-IV, mat A
ΔFRQ	DBP1320	NCU02265	Δ*frq::bar*$^{+}$; mat a
RPS19-V5 Heterokaryon	DBP2675	NCU07826	*rps19*::6xGly-V5::*hph,* mat A
RPS19-V5	DBP2754	NCU07826	*rps19*::6xGly-V5::*hph,* mat A, homokaryon
RPL27-V5 Heterokaryon	DBP2678	NCU01827	*rpl27*::6xGly-V5::*hph.* mat A
RPL27-V5	DBP2720	NCU01827	*rpl27*::6xGly-V5::*hph,* mat A, homokaryon
RPL25-FLAG	DBP2512	NCU06226	Δ*rpl25*::*hph*; *his3*$^{+}$::*rpl25*::FLAG-His6x, mat a
RPL27-V5; RPL25-FLAG	DBP2825	NCU01827 x NCU06226	Δ*rpl25*::*hph*; *his3*$^{+}$::*rpl25*::FLAG-His6x; *rpl27*::6xGly-V5::*hph*

Table 2. Nomenclature for strains used in this study.

2.2 Germinated conidia time courses

Germinated conidia time courses were carried out as follows: Conidia was harvested after 7 days of growth (30°C in constant light, LL) from 250 mL Erlenmeyer flasks containing 100 mL of VM plus 1.5% agar. Cell counts for germinated conidia were determined using 8 µL of a 1:200 dilution of the conidial suspension on a hemocytometer slide (Curtin Matheson Scientific, Houston, TX) using a Leitz Laborlux S microscope (Leica microsystems). 1 L Erlenmeyer flasks containing 500 mL of VM liquid were inoculated with 1 x 10^5 conidia per mL for DD 12-32 timepoints, and with 1 x 10^4 conidia per mL for DD 36-44 timepoints. The flasks were grown at 25°C LL with shaking (100 rpm) and were subsequently transferred to 25°C DD at the appropriate times as indicated in Figure 5.

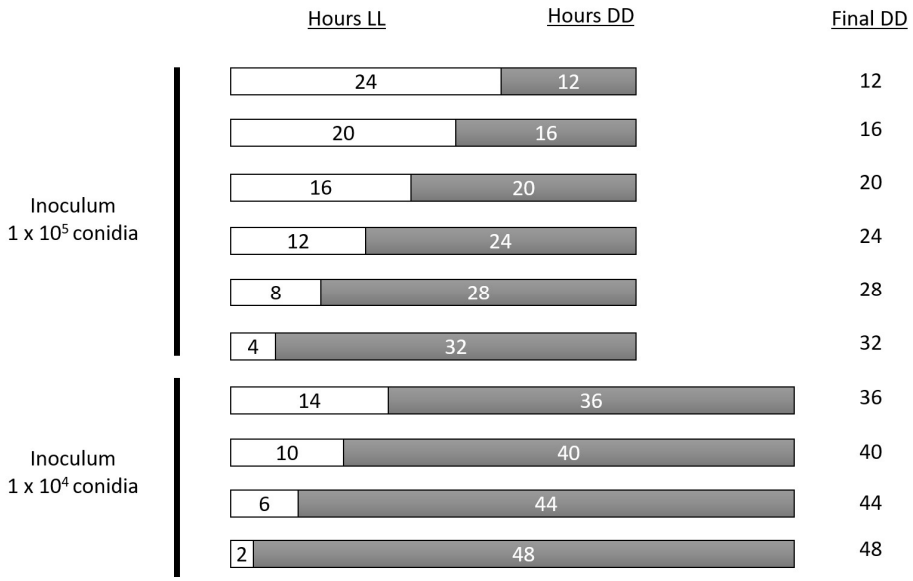

Figure 5. Schematic representation of germinated conidia time course culture growth time in hours LL and DD. LL is represented as white bars and DD is represented as gray bars. The hours in LL and DD are indicated in the white and grey bars for each time point collected (final DD).

The germinated conidia were harvested using vacuum filtration over hardened ash-less Whatman filter paper (GE Healthcare, Life Sciences, Marlborough, MA) and rinsed with ice cold sterile water. Once harvested, the samples were cut into squares about 1 cm x 1 cm, frozen in liquid nitrogen, and stored at -80°C until use.

2.3 Generation of V5-tagged and dual-tagged ribosomal protein (RP-V5 and RPL25-FLAG) strains

N. crassa carrying C-terminal V5-tagged RPS19 (DBP2754, *rps19*(NCU07826)::6xGly::V5::*hph*) and RPL27 (DBP2720, *rpl27*(NCU01827)::6xGly::V5::*hph*) were generated via fusion PCR and homologous recombination. Briefly, genomic DNA from WT *N. crassa* was amplified by PCR, using Phusion taq (ThermoFisher Scientific, Walthman, WA) and the indicated primers in Table 3, to generate a 1 kb 5' flank and ORF of the specific ribosomal protein (fragment 1), and a 1 kb 3' flank of the ribosomal protein (fragment 3). Fragment 2, which contains the epitope-tag and a hygromycin resistance cassette was amplified from plasmid pDBP525 [15, 57] to contain the 1.8 kb fragment, 6xGLY::V5::*hph* flanked by 20-30 bp of homology to *rps19* or *rpl27* (Table 3). The PCR products were purified by QIAquick PCR Purification Kit (Qiagen, Hilden, Germany). The three fragments were fused together using 3-way fusion PCR, creating a full fragment containing the 5' flank and ORF, 6xGLY::V5::*hph*, and the 3' flank (Figure 6). The final fusion constructs were purified by gel extraction using the QIAquick Gel Extraction Kit (Qiagen, Hilden, Germany), and 300-500 ng were transformed into WT *N. crassa* cells by electroporation [4, 34, 41]. Transformants that grew on hygromycin selection plates were first screened by western blot with anti-V5 antibody (Invitrogen #R960-25) to determine if they

expressed a tagged-protein of the expected size. Confirmation that the insertions occurred at the endogenous *rps19* and *rpl27* loci was performed by PCR with primers (Table 3) used to generate fragment 2 and outside the regions of homologous recombination (Figure 6). Strains with appropriate integration were stored: DBP2675 (RPS19-V5 heterokaryon, *rps19*::6xGly-V5::*hph*, mat A) and DBP2678 (RPL27-V5 heterokaryon, *rpl27*::6xGly-V5::*hph*, mat A).

Fragment	Forward/Reverse Primer	DBP Number	Primer Sequence
Primers to create epitope tag RPS19-V5			
Fragment 1F	Forward	28-16	5' ACCATTGGTTCAATGATGCA 3'
Fragment 1R	Reverse	28-17	5' TCCGCCGCCTCCCTCGTCATCCTCCTCATCAG 3'
Fragment 2F	Forward	28-18	5' GAGGATGACGAGGGAGGCGGCGGAGGCGGTAAG 3'
Fragment 2R	Reverse	28-19	5' CTAGCGACGAATACTTCCGAGCTCGGATCCAT 3'
Fragment 3F	Forward	28-20	5' GAGCTCGGAAGTATTCGTCGCTAGATATCATG 3'
Fragment 3R	Reverse	28-21	5' TTGCTTCTCAATACTGTCAT 3'
Primers to check for homologous recombination of RPS19-V5			
Outside homology 5'	Forward	29-50	5' GAGAGCGGGAATGTCGTTTC 3'
Outside homology 3'	Reverse	29-51	5' GGACTGCGAACGGAATGGTT 3'
Primers to create epitope tag RPL27-V5			
Fragment 1F	Forward	28-4	5' TCTCGCTCCTGACCCCTGCC 3'
Fragment 1R	Reverse	28-5	5' TCCGCCGCCTCCGAAACCTAAAGATGCAGGGT 3'
Fragment 2F	Forward	28-6	5' TCTTTAGGTTTCGGAGGCGGCGGAGGCGGTAAG 3'
Fragment 2R	Reverse	28-7	5' TAGAAGACTAATACTTCCGAGCTCGGATCCAT 3'
Fragment 3F	Forward	28-8	5' GAGCTCGGAAGTATTAGTCTTCTACTCTCGGT 3'
Fragment 3R	Reverse	28-9	5' GCAGAGAGAGAAAGTGGGCA 3'
Primers to check for homologous recombination of RPL27-V5			
Outside homology 5'	Forward	29-79	5' GAGTACGATCCCGCCCGGATAG 3'
Outside homology 3'	Reverse	29-80	5' TCATCTTCTCTAGCCAGGTCAT 3'
Primers to check for endogenous Δ*rpl25*			
Outside 5’	Forward	32-37	5' CGTCAATTTCTTCAAGGAGGCG 3'
Outside 3’	Reverse	32-38	5' CAATGGATATTCCTCAGGCCGA 3'

Table 3. Primers used to generate and validate homologous recombination of ribosomal protein V5-epitope tag.

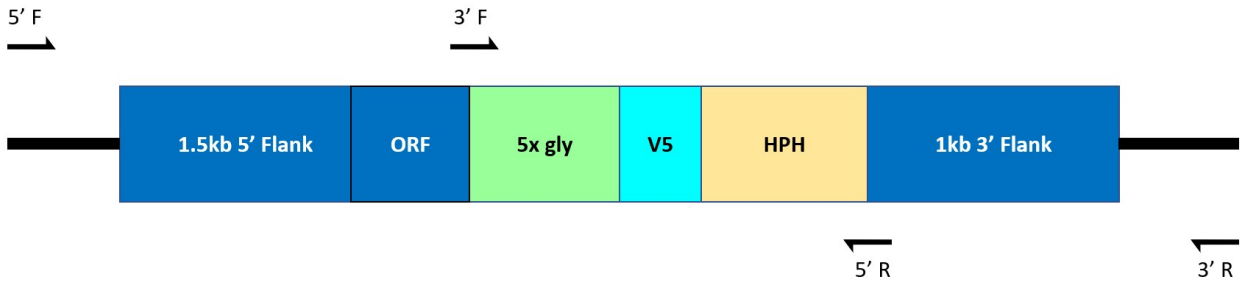

Figure 6. V5 tagging strategy for validation of predicted rhythmic ribosomal proteins. To verify homologous recombination, 5' F and 5' R primers (DBP 29-79 and DBP 28-7; DBP 29-50 and DBP 28-19) and 3' F and 3' R primers (DBP 29-80 and DBP 28-6; DBP 29-51 and DBP 28-18) were used to check for 5' and 3' integration of RPL27-V5 and RPS19-V5 respectively. Primers are listed in Table 3.

To obtain homokaryons, the RPS19-V5 and RPL27-V5 heterokaryons, were crossed to RPL25-FLAG using standard protocols [14]. Cross progeny were screened for hygromycin resistance indicating a RP-V5::*hph* or Δ*rpl25*::*hph* genotype. The progeny were screened by western blot for the presence of the V5 and FLAG tags, and homokaryotic strains which contained only the V5-epitope tag, and not RPL25-FLAG or *Δrpl25*::*hph*, were stored: DBP2720 (RPL27-V5, *rpl27*::6xGly-V5::*hph*, mat A) and DBP2754 (RPS19-V5, *rps19*::6xGly-V5::*hph*, mat A).

To obtain a dual-tagged strain, progeny from a cross between RPL27-V5 (DBP2720) and RPL25-FLAG (DBP2512) were screened by western blot with anti-V5 and anti-FLAG antibody. Strains which contained both the V5 and FLAG tags were then analyzed for the presence of Δ*rpl25*::*hph* as follows: The *rpl25* locus was amplified via PCR using the primers presented in Table 3. The amplified product was digested with Stu1, which only cuts the endogenous WT *rpl25*, and with EcoR1, which cuts the hygromycin-B cassette contained in the Δ*rpl25*::*hph*

(NEB, Ipswich, Massachusetts). Strains that contained the dual tag and Δ*rpl25*::*hph* were stored: DBP2825 (Δ*rpl25(*NCU06226)::*hph*; *his3*$^{+}$::*rpl25*::FLAG-His6x; *rpl27*(NCU01827)::6xGly-V5::*hph*).

2.4 Protein extraction and western blots

To validate that the RPL27-V5 and RPS19-V5 cultures were rhythmic, total protein was extracted with a modified extraction buffer (50 mM HEPES, 137 mM NaCl, 10% glycerol, 1 mM EDTA, 10 mM NaF, 1 mM β-glycerophosphate, 1 mM Na-orthoranodate, and 1 mM PMSF) and analyzed for FRQ protein abundance by western blot [20]. 100 µg of the protein extracts were separated on an 10% SDS-PAGE and transferred to an Immobilon-P PVDF transfer membrane with 0.45 µm pore size (Sigma-Aldrich, St. Louis, MO) at 100 V for 1 hour at 4°C. The membranes were blocked overnight at 4°C in 7.5% non-fat dry milk with 1x TBS and 0.1% Tween-20 (1x TBST). The membranes were then probed with anti-FRQ monoclonal primary antibody (mFRQ3G11, from M. Brunner's laboratory, Heidelberg) at a 1:200 concentration in 7.5% non-fat dry milk in 1x TBST, and probed overnight at 4°C. After primary antibody incubation, membranes were washed 6 times in 1x TBST for 10 minutes and probed with secondary antibody overnight at 4°C. The secondary antibody was goat anti-mouse IgG HRP secondary antibody (Bio-Rad, Hercules, CA) used at a concentration of 1:10000 in 7.5% non-fat dry milk in 1x TBST. After secondary incubation, membranes were washed 6 times in 1x TBST for 10 minutes and FRQ protein was detected with Super Signal West Femto Maximum Sensitivity Substrate (Thermo Scientific, Walthman, MA) using autoradiography with Premium x-ray film (Phenix research products, Candler, NC).

For the validation of the FLAG and V5-epitope tagged strains, the protein extraction procedure was identical to the FRQ extraction described above with the addition of the protease inhibitors 1 µg/mL aprotinin, 1 µg/mL pepstatin A, and 1 µg/mL leupeptin (Sigma-Aldrich, St. Louis, MO). Anti-V5 primary antibody (Invitrogen #R960-25, Waltham, MA) was used according to manufacturer recommendation, probed with secondary antibody, goat anti-mouse IgG HRP (Bio-Rad, Hercules, CA), and signal was detected with the Super Signal West Pico Plus Substrate (Thermo Scientific, Walthman, MA). The primary anti-FLAG antibody (Cell Signaling Technology #2368, Beverly, MA) was used according to manufacturers recommended protocol and was probed with secondary antibody, goat anti-rabbit IgG HRP Conjugate (Bio-Rad, Hercules, CA) and detected using Super Signal West Pico Plus Substrate.

The pelleted ribosome western blots were performed as above on a 15% SDS-PAGE gel with 100-150 µg of protein loaded, as determined through NanoDrop, and probed with anti-V5 antibody.

2.5 Sucrose density centrifugation for pelleted ribosome isolation

The germinated time courses samples from RPL27-V5 and RPS19-V5 strains were subject to sucrose density centrifugation to pellet the ribosomes as previously described with modifications [23, 24]. 1 g of the germinated conidia samples were cryogenically ground in SPEX SamplePrep 6850 Freezer/Mill with 1 mL of frozen lysis buffer beads (20 mM Tris-Cl [pH 7.5], 150 mM NaCl, 5 mM $MgCl_2$, 1 mM DDT, 1% Triton X-100, 25 U/mL Turbo DNase [Invitrogen, AM2238, Waltham, MA], 100 µg/mL cycloheximide [Sigma-Aldrich, St. Louis, MO], in DEPC [Aldrich Chemistry, St. Louis, MO] treated water), which were placed into pre-chilled grinding vials. The settings of the freezer-mill were 10 minutes of pre-cooling, with three two-minute

grinding cycles, separated by a one-minute re-cooling between each cycle. The resultant powdered cell extracts were transferred to pre-chilled 50 mL polycarbonate centrifuge tubes, thawed in an ice-bath for 30 minutes, and centrifuged for 15 minutes (16,000 rpm, at 4°C in an SS34 rotor). 1 mL of the supernatant was collected and placed in new 2.0 mL microcentrifuge tube and maintained on ice. The A_{260} and A_{280} of a 200-fold dilution was measured using Bio UV-visible spectrophotometer (Varian, Walnut Creek, CA). 50 A_{260} units per sample were brought up to a volume of 300 µL with lysis buffer and treated with 1.875 µL of RNaseI (Invitrogen, AM2294, Waltham, MA) for 45 minutes at room temperature on a Nutator. Following incubation, the digestion was transferred to a pre-chilled 13 mm x 51 mm polycarbonate ultracentrifuge tube (Beckman Coulter, Brea, CA). To pellet the ribosomes, a 900 µL underlay of 1 M sucrose cushion (20 mM Tris-Cl pH 7.5, 150 mM NaCl, 5 mM $MgCl_2$, 1 mM DDT, 100 µg/mL cycloheximide, and 34% sucrose in DEPC treated water) was carefully dispensed into the polycarbonate tube. The polycarbonate ultracentrifuge tubes were loaded into a pre-cooled TLA100.3 rotor and centrifuged at 4°C for 4 hours at 70,000 rpm. Following centrifugation, the outside edge of the centrifuge tube was marked to note the location of the ribosome pellet before removing the tube from the rotor. The supernatant was then carefully pipetted out and the pellet was resuspended in 400 µL of DEPC treated water and separated out into four 100 µL aliquots, which were frozen in liquid nitrogen and stored at -80°C until use.

2.6 Sucrose density gradient fractionation and profile analysis

To determine the effect of the circadian clock and the epitope tags on individual components of ribosomes, sucrose density gradient fractionation was performed on WT, RPL25-FLAG, and RPL27-V5; RPL25-FLAG extracts. Samples were extracted as previously described, with minor

changes [40]: Germinated conidia from DD12 and DD24 timepoints were treated with 100 µg/mL of cycloheximide 5 minutes prior to harvest. 0.5 g of wet weight of the sample was added to 2 mL microcentrifuge screw cap tubes containing 1.5 mL of polysome extraction buffer (100 mM KCl, 20 mM HEPES-KOH [pH 7.5], 10 mM $Mg_3(PO_4)_2$, 15 mM 2-mercaptoethanol [BME, Sigma-Aldrich, St. Louis, MO], and 100 µg/mL of cycloheximide) and 0.5 g of 0.5 mm Zirconia beads (BioSpec Products, Bartlesville, OK). The cells were disrupted in a bead-beater at 4°C for 50 seconds and centrifuged at 4°C for 5 minutes at 13,200 rpm. 900 µL of the supernatant was transferred to a fresh 1.5 mL microcentrifuge tube, an A_{260} measurement was taken, and 250 µL of 50% glycerol and 100 µL of 50 mg/mL heparin (Sigma-Aldrich, St. Louis, MO) was added. The samples were then frozen in liquid nitrogen and stored at -80°C until use.

The sucrose gradient was made using BIOCOMP Gradient Station. A stock 60% sucrose solution (DEPC treated sterile water and filter sterilized) and a 10x polysome gradient buffer (100 mM HEPES-KOH, 700 mM NH_4OAc, and 50 mM $Mg(OAc)_2$, all solutions made in DEPC water and filter sterilized), were used to generate 10% and 50% sucrose gradient solutions (each containing 1x polysome gradient buffer). The 10% sucrose gradient solution was pipetted into open-top polyclear centrifuge SW41 14 x 89 mm tubes (Seton, Petaluma, CA) until halfway up the tube length (about 7.5 mL), which was denoted by a mark using the marking cylinder. The 50% sucrose solution was added (about 7 mL) via a long needle syringe to underlie the 10% solution until the centrifuge tube was slightly over filled. The 10-50% linear gradients were generated in the centrifuge tubes containing sucrose solutions using the BIOCOMP Gradient Station and chilled at 4°C for minimum of 45 minutes to maximum of 3 days.

Extracts were thawed and 10 to 20 A_{260} units (in a volume not exceeding 300 µl) were layered on-top of the 13 mL linear 10-50% sucrose gradient. Centrifuge tubes were balanced

within 0.05 g and centrifuged in a SW41 rotor at 41,000 rpm for 2 hours at 4°C with deceleration set at coast in a Beckman Coulter Optima XE-90 Ultracentrifuge (Beckman Coulter, Brea, CA).

Using the TRiAX Flow Cell Program and Gilson Fraction Collector (Middleton, WI), fractions were collected in 26 fractions containing 0.5 mL each, and were collected starting from the top of the gradient (low density) with a continuous A_{260} measurement. Following fractionation, samples were collected and quickly frozen in liquid nitrogen and stored at -80°C for further analysis.

To quantitate the sucrose density gradient profiles generated from the different samples, the minimum A_{260} absorbance in each profile was set to zero, since there was run to run variation in this value. The absorbance values under the curve of the 40S, 60S, 80S, polysome fractions, and the total of the sucrose density gradient profile, were individually determined. The individual fractions sums were then divided by the sum of the total absorbance of the profile to obtain the percentage of the individual components of the sucrose density gradient profile.

3. RESULTS

3.1 Generation of ribosomal protein-tagged strains

While MS/MS data suggested that there are 15 ribosomal proteins with rhythmic abundance in the ribosomes, we wished to validate rhythmicity of these proteins in independent experiments. I first focused two ribosomal proteins predicted to be rhythmic in both the TAMU and EMSL data sets (RPL27 and RPS19). Because no commercial antibodies were available, these ribosomal proteins were V5-epitope-tagged at their C-terminus and transformed back to their native loci by homologous recombination (Figure 6). To confirm proper integration of the V5-tag, colonies were screened by PCR using the primers indicated (Table 3). Positive transformants of both RPL27-V5 (Figure 7) and RPS-19-V5 were obtained (Figure 8). Transformant #2 (DBP2678) showed the predicted 5' and 3' validation fragments for RPL27-V5 integration (Figure 7). While both transformant #2 and #3 showed the predicted 5' and 3' validation fragments for RPS19-V5 integration (Figure 8), only #2 was stored (DBP2675). These progenies were sexually crossed to RPL25-FLAG to obtain homokaryons which contain only the V5-epitope tag. The progeny of these crosses were screened through western blot with both anti-V5 and anti-FLAG antibody (Figure 9). RPL27-V5 transformant #1 (DBP2720) and RPS19-V5 transformant #1 (DBP2754), which contained only V5-tagged protein, and not RPL25-FLAG tagged protein, were stored for further studies (Figure 9). These epitope tagged ribosomal proteins supported growth, and are at least partially functional, since they are able to be obtained as homokaryons and exhibit WT growth on selective slants.

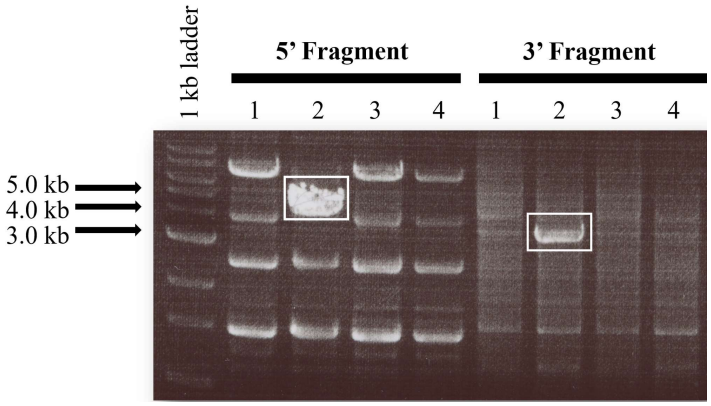

Figure 7. Validation of correct integration into the endogenous locus for RPL27-V5 tag. Agarose gel electrophoresis (1% agarose) of PCR amplified products to screen for proper homologous recombination. The gel was stained with ethidium bromide and DNA was visualized using UV absorption. Three possible transformants of RPL27-V5 (Lanes 1, 2, and 3) and a WT negative control (lane 4) were screened for proper integration into the endogenous locus with a 5' validation fragment (4239 bp) and 3' validation fragment (3470 bp). Transformant #2, boxed, shows the correct size for integration of both the 5' and 3' end. Non-specific bands are seen in transformants, and the WT control #4.

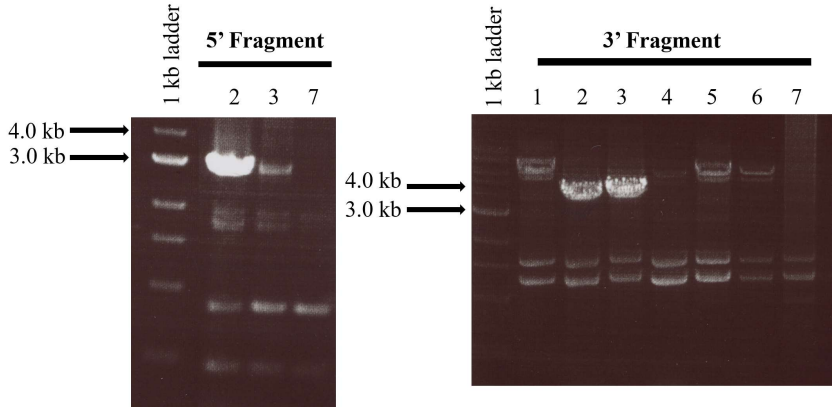

Figure 8. Validation of correct integration into the endogenous locus for RPS19-V5 tag. Agarose gel electrophoresis (1% agarose) of PCR amplified products to screen for proper homologous recombination. The gels were stained with ethidium bromide, and DNA was visualized using UV absorption. Six possible transformants (left; lanes 1-6) of RPS19V5 were screened for 3' integration (3867 bp), and two possible transformants (right; lanes 2 and 3) were screened for 5' integration (3047 bp), both with a WT negative control (lane 7). Transformants #2 and #3, boxed, show the correct size for integration of both 5' and 3' homology. Non-specific bands are seen in transformant, and the WT control #7.

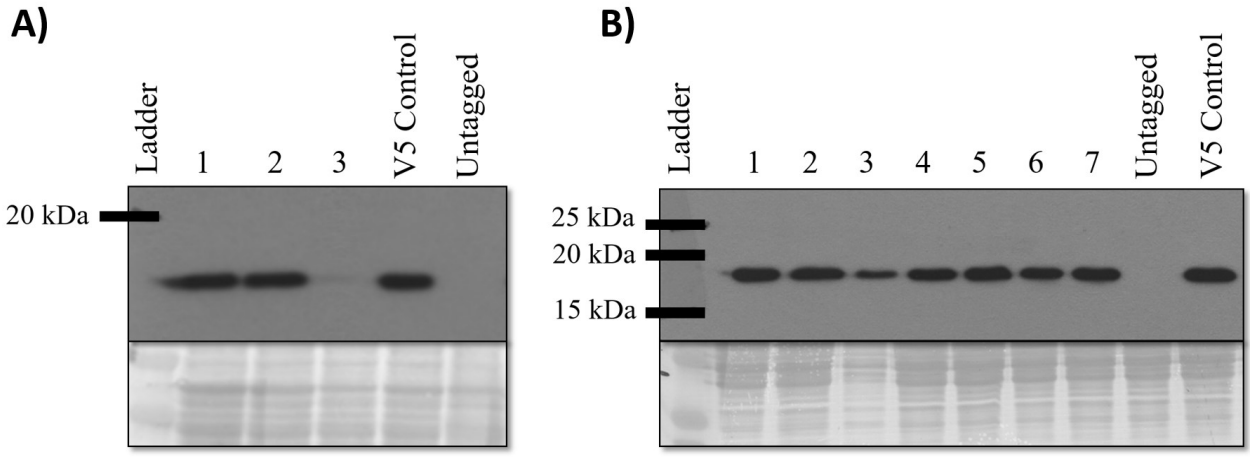

Figure 9. RPL27-V5 and RPS19-V5 homokaryon progeny tag validation. (A) RPL27-V5 protein in total extracts were analyzed by western blot and probed with anti-V5 antibody. A band close to the predicted size of the protein, 17.1 kDa is observed in two of the three possible progeny, lanes 1 and 2. (B) RPS19-V5 protein in total extracts was analyzed by western blot and probed with anti-V5 antibody. A band close to the predicted size of the protein,18.1 kDa, is observed in all of the progeny, (lanes 1-7). Specificity of the V5 antibody was demonstrated by comparing WT untagged and V5-tagged controls extracts. Amido black stained membranes were used to ensure equal loading in A and B.

3.2 Generation of RPL27-V5; RPL25-FLAG dual-tagged strain

In addition to the single V5-epitope tagged strains, I generated a dual-tagged strain containing RPL27-V5 and RPL25-FLAG tag. Because RPL25 levels are not rhythmic in ribosomes, this serves as an internal arrhythmic control. The RPL27-V5 (DBP2720) homokaryon was sexually crossed with RPL25-FLAG (DBP2512) to generate the dual-tagged strain. The progeny were screened by western blot to obtain strains that contain both the V5 and FLAG tags (Figure 10). In addition, progeny which were positive for both tags were screened to ensure that they contained Δ*rpl25*::*hph* at the endogenous locus. PCR was performed on genomic DNA with primers flanking the native *rpl25* locus, and because the deletion and WT fragments are of similar size,

the PCR products were distinguished by restriction digestion. EcoR1 cuts within the hygromycin-B cassette of PCR products derived from Δ*rpl25*::*hph* progeny, as well as in the RPL25-FLAG; Δ*rpl25*::*hph* control (Figure 11). Stu1 cuts within the WT *rpl25*$^{+}$ PCR product, and only shows up in the WT984 control (Figure 11). Progeny #1 (DBP2825) and progeny #2 (DBP2826) both contained Δ*rpl25*::*hph* and were stored; DBP2825 was used in further experiments. The viability of the dual tagged RPL27-V5; RPL25-FLAG homokaryons suggested that dual-tagged ribosomes are capable of sufficient translation to support growth.

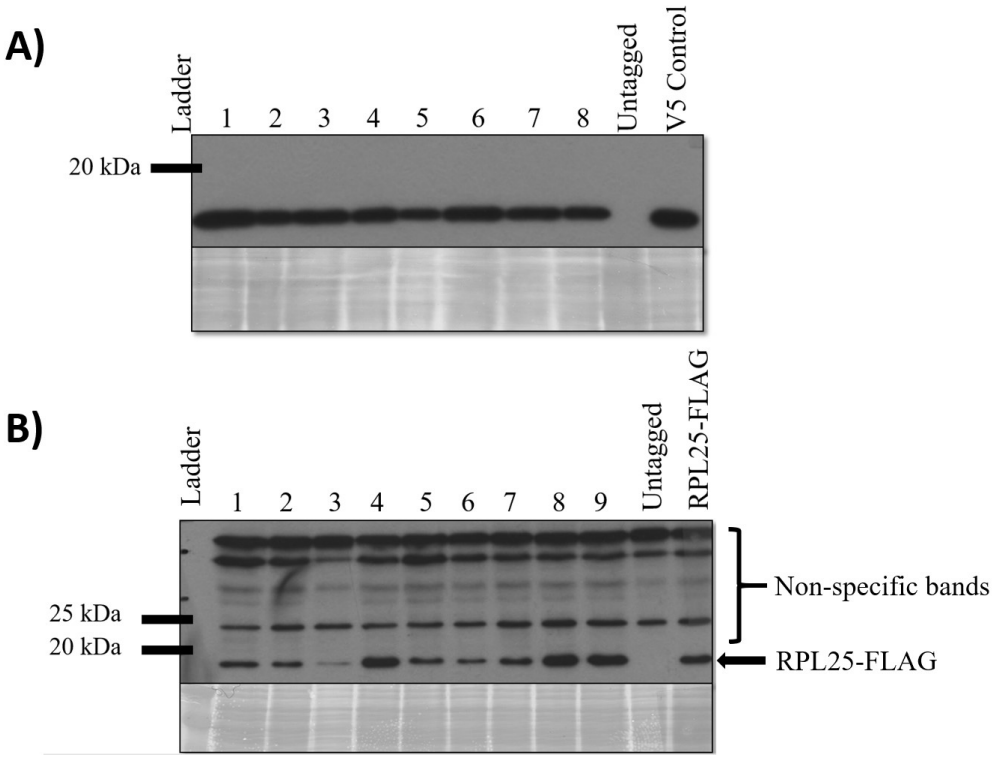

Figure 10. Generation of RPL27-V5; RPL25-FLAG dual tag. Progeny of a sexual cross between RPL27-V5 and RPL25-FLAG were analyzed by western blot and probed with anti-V5 antibody (A) and anti-FLAG antibody (B). (A) RPL27-V5 is observed near the predicted size of 17.1 kDa in progeny 1-8 (lanes 1-8) and (B) RPL25-FLAG is observed near the predicted size of 18.9 kDa in all progeny (lanes 1-9) with non-specific bands seen in all progeny (lanes 1-9), RPL25-FLAG, and untagged control. Amido black stained membranes were used to ensure equal loading.

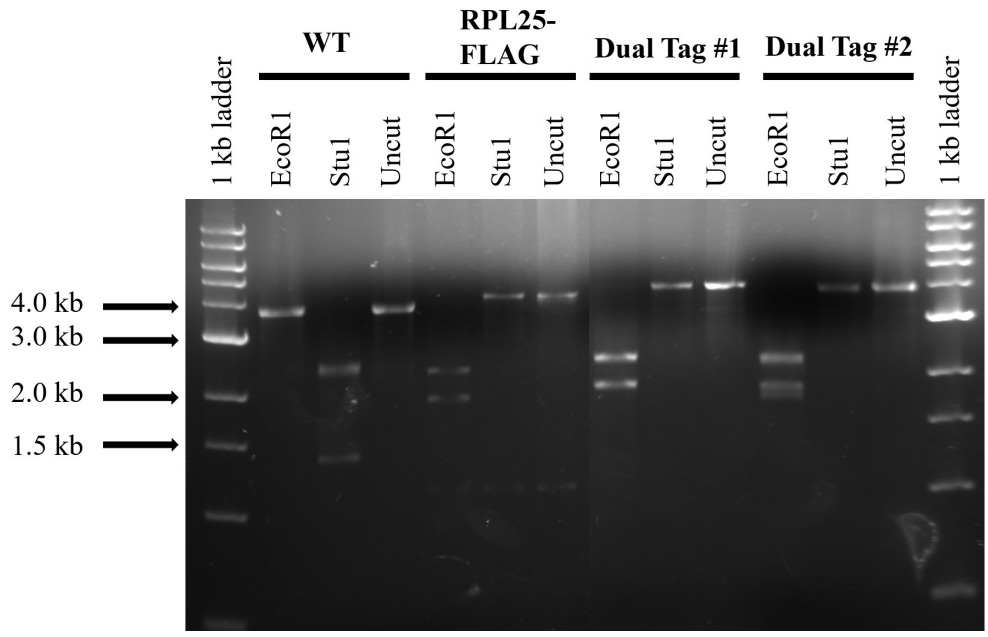

Figure 11. Restriction enzyme digest to ensure Δ*rpl25::hph* is present at the endogenous locus in RPL27-V5; RPL25-FLAG strains. Stu1 cuts WT PCR products and EcoR1 cuts Δ*rpl25* PCR products. EcoR1 is shown to cut RPL25-FLAG and dual-tagged strain 1 and 2, and exhibits two bands (2278bp, 1914bp). Stu1 is shown to cut WT PCR products, but not the RPL25-FLAG or dual-tagged strains, and exhibits two bands (2483bp, 1549bp).

3.3 Pelleted ribosomes do not show a rhythm in RPL27-V5 incorporation

To examine rhythmicity of RPL27-V5 in ribosomes, germinated conidia from four independent time courses (harvested every 4 hours from DD12 to DD48) were cryogenically ground and pelleted in a sucrose cushion to enrich for ribosomes. This method was performed to ensure similarity to the mass spectroscopy sample preparation. To confirm that normal rhythmicity of the circadian oscillator was displayed in the time courses, FRQ levels were examined by western blot. Figure 11 shows that the RPL27-V5 tagged strains display normal FRQ protein rhythmicity ($p<0.0001$), with a peak at DD20 and DD40 and a phosphorylation profile similar to previous studies [20, 39]. These data suggested that the clock was functional in this strain. Unlike the

mass spectroscopy data predicting RPL27 levels to be rhythmic in ribosomes, RPL27-V5 was arrhythmic in these independent experiments (Figure 12). It is possible that the V5 tag and hygromycin B cassette interfered with the normal rhythmic regulation of RPL27. Examination of a time course of pelleted ribosomes from a WT untagged strain using an anti-RPL27 antibody would solve this potential problem; however, currently there are no such antibodies available.

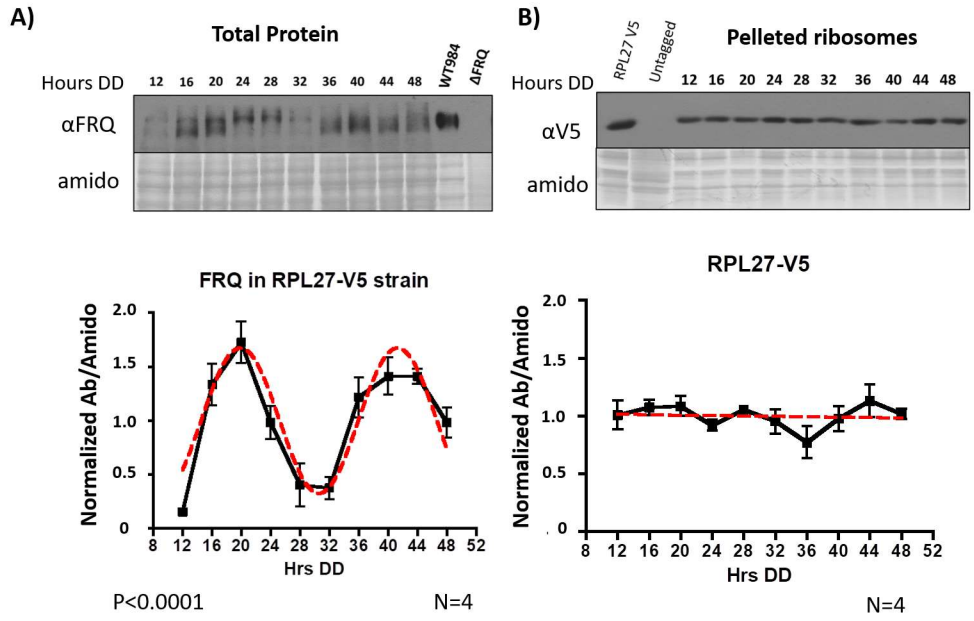

Figure 12. RPL27-V5 is arrhythmic in rhythmic germinated conidia cultures. A) FRQ protein levels in total extracts from cells harvested at the indicated times (hours) in DD were analyzed by western blot, and even loading of the protein samples was confirmed by amido black staining of the membrane (top panel). Specificity of the FRQ antibody was demonstrated by comparing WT untagged extracts and ΔFRQ samples. B) RPL27-V5 protein levels in pelleted ribosomes were analyzed by western blot and probed with anti-V5 antibody. Amido black stained membranes were used to normalize protein loading. Specificity of the V5 antibody was demonstrated by comparing WT untagged extracts and a V5-tagged sample. The data, plotted below (mean ± SEM, n=4), show FRQ protein levels are rhythmic (A) as confirmed by F-test of fits to a sine wave, dotted line ($p<0.0001$), and RPL27-V5 pelleted ribosome levels are arrhythmic (B) as confirmed by F-test of best fits to a line.

3.4 Pelleted ribosomes do not show a rhythm in RPS19-V5 incorporation

To examine rhythmicity of RPS19-V5 in ribosomes, pelleted ribosomal proteins were examined from three independent time courses as described for RPL27-V5 above. To ensure that the time courses displayed normal rhythmicity, FRQ levels were examined by western blot. Figure 12 shows that the RPS19-V5 tagged strains display normal FRQ protein rhythmicity and phosphorylation [20, 39] ($p<0.0001$), suggesting that the clock functioned normally in this strain. Despite a functional clock, RPS19-V5 in pelleted ribosomes was arrhythmic (Figure 13, n=3).

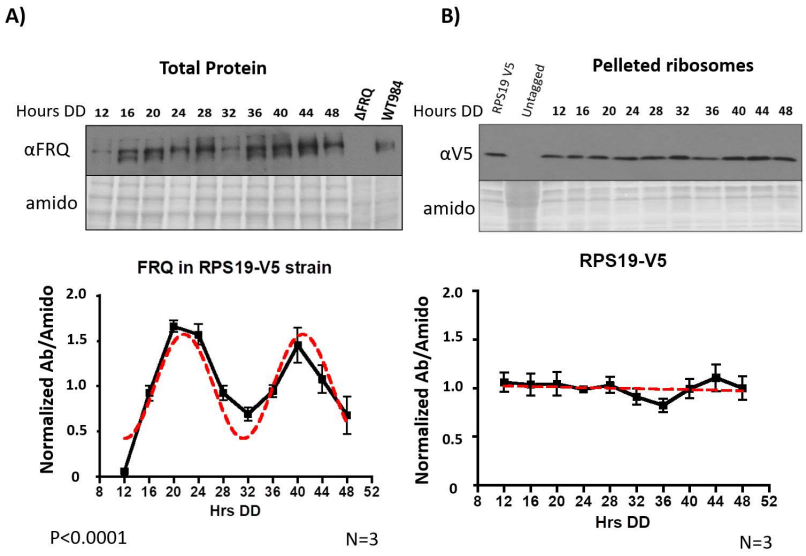

Figure 13. RPS19-V5 is arrhythmic in rhythmic germinated conidia cultures. A) FRQ protein levels in total extracts from cells harvested at the indicated times (hours) in DD were analyzed by western blot, and even loading of the protein samples was confirmed by amido black staining of the membrane (top panel). Specificity of the FRQ antibody was demonstrated by comparing WT untagged extracts and ΔFRQ samples. B) RPS19-V5 protein levels in pelleted ribosomes were analyzed by western blot and probed with anti-V5 antibody. Amido black stained membranes were used to normalize protein loading. Specificity of the V5 antibody was demonstrated by comparing WT untagged extracts and a V5-tagged sample. The data, plotted below (mean ± SEM, n=3), show FRQ protein levels are rhythmic (A) as confirmed by F-test of fits to a sin ewave, dotted line ($p<0.0001$), and RPS19-V5 pelleted ribosome levels are arrhythmic (B) as confirmed by F-test of best fits to a line.

However, when looking at the individual replicates for RPS19-V5, (Figure 14 A-C), the peak and trough of replicates 1 and 2 share similarities, and when they are averaged together (Figure 14D), the shape of the plot (Figure 14D) resembles that of the MS/MS data shown in Figure 14E. This suggests the possibility of a low amplitude rhythm for RPS19-V5, and identifies the need to perform more replicates to be confident of the data. In addition, the same problem may exist with the epitope tag and hygromycin B cassette interfering with rhythmic control as described above for RPL27, and again, there is currently no antibody available against RPS19 to circumvent this problem.

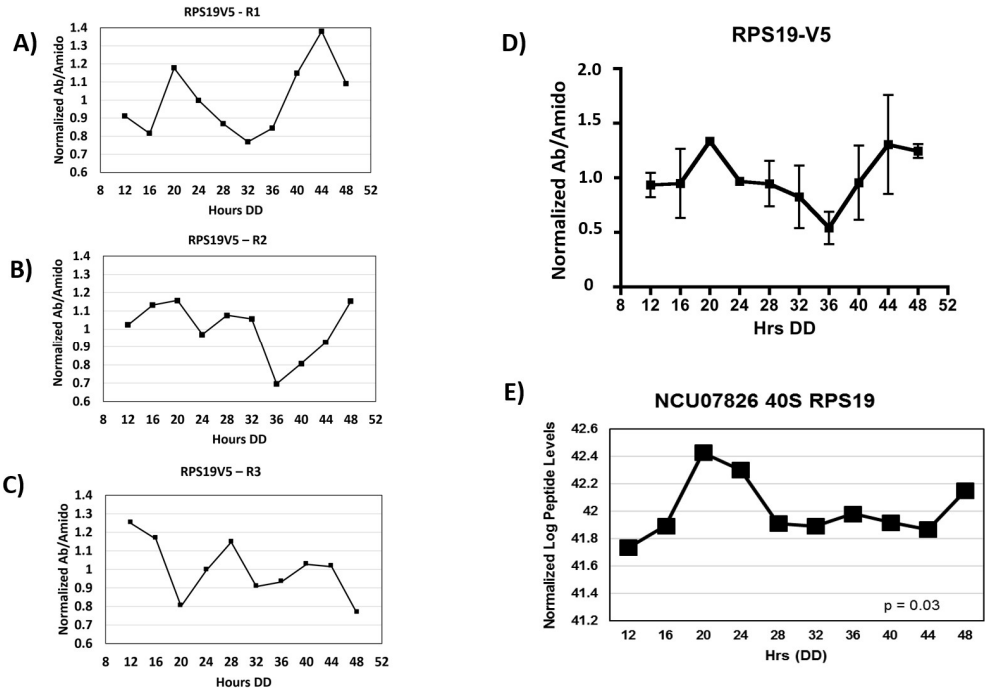

Figure 14. Circadian regulation of individual replicates of RPS19-V5 pelleted ribosomes. (A), (B), and (C) show individual replicates of pelleted ribosomes isolated from RPS19-V5 cells harvested at the indicated times (hours) in DD. (D) Average of replicate 1 and 2 (A and B), shows a low amplitude rhythm, with peak at DD20 and trough at DD36. The graph shows the average signal normalized to total protein loaded. (E) MS/MS data plot of RPS19 from EMSL, normalized log peptide levels are plotted. (D) Values are mean ± SEM, n=2.

3.5 The fraction of translating ribosomes or ribosomal subunits is similar at DD12 and DD24 in WT cells

To examine if translation is preferentially occurring at night, the time of day when energy levels are high, and eEF2 and eIF2α are active in *N. crassa* (S. Karki unpublished) [7], I determined if there was a time-of-day difference in the abundance of RNA associating with ribosomal components in a WT strain at DD12 (subjective morning) and DD24 (subjective evening). Cell extracts were loaded onto a sucrose density gradient to separate 40S and 60S ribosomal subunits, 80S monosomes, and higher density polysomes, into multiple fractions. Figure 15 shows that the sucrose density gradient profiles of a WT strain had no apparent time-of-day difference in the ratio of their subunits and individual components. While all gradients were loaded with the same amount of A_{260}, gradients may have received differing volumes of sample, which may account for the difference in overall absorbance between timepoints. Quantitation of the area under the component peaks confirmed that there is little to no difference in the ratio of the subunits between DD12 and DD24 (Figure 16A). To confirm and extend these findings, more timepoints should be examined to get a more complete picture of possible circadian-regulated translation.

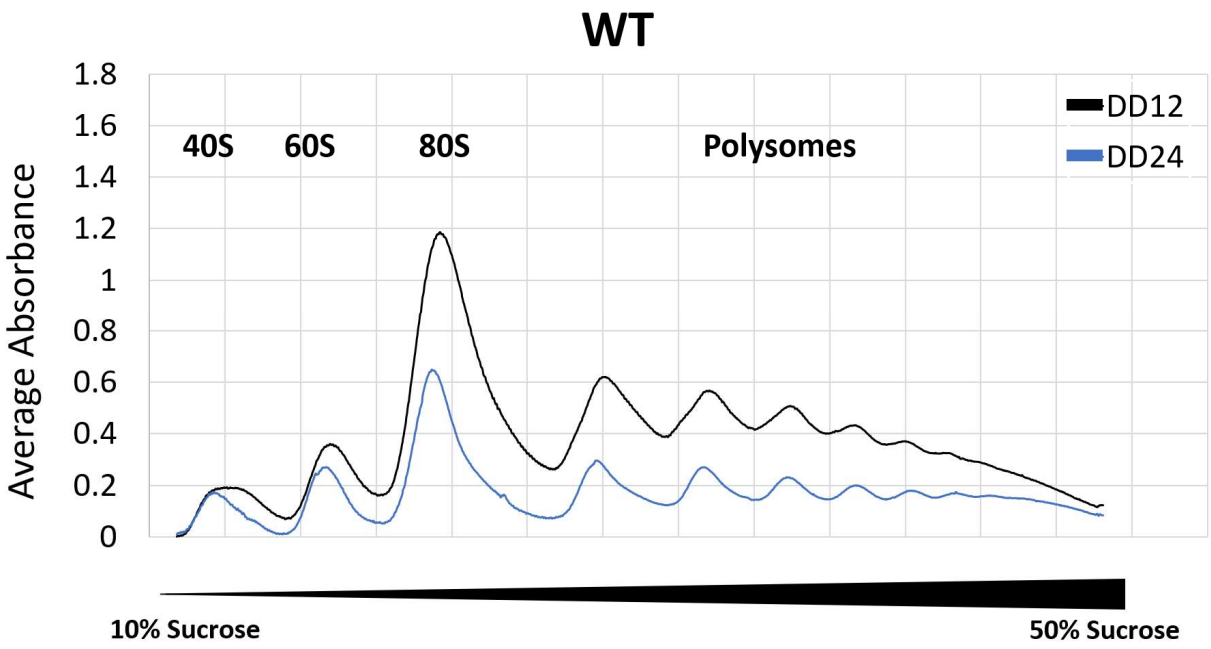

Figure 15. Average sucrose density gradient profile of WT cells at two different time points, DD12 and DD24. Profile was normalized to 0; n=2.

3.6 Ribosomal protein tags weakly influence ribosome subunit abundance

To determine the effect of the epitope tags on the ribosomal fraction abundance, I examined sucrose density gradients of the RPL25-FLAG strain (Figure 17) and the dual-tagged RPL27-V5; RPL25-FLAG strain (Figure 18), at DD12 and DD24. RPL25-FLAG profiles showed no apparent time-of-day difference comparing DD12 and DD24 (Figure 16B). However, there is a time-of-day difference in both the 80S monosome and in the polysomes in the dual-tagged strain (Figure 16C). When comparing the ratios of the ribosome fractions from the WT untagged strain to the single or dual-tagged strain, there is a difference in the composition at DD12 (Figure 16). The tags progressively decrease the amount of polysomes from 59% in WT cells, to 48% in dual-

tagged cells at DD12 (Figure 16). However, more replicates are needed to determine if this change is significant. In any case, these data suggested the possibility that epitope tagging the ribosomal proteins may interfere with proper ribosome structure and have a negative impact on translation.

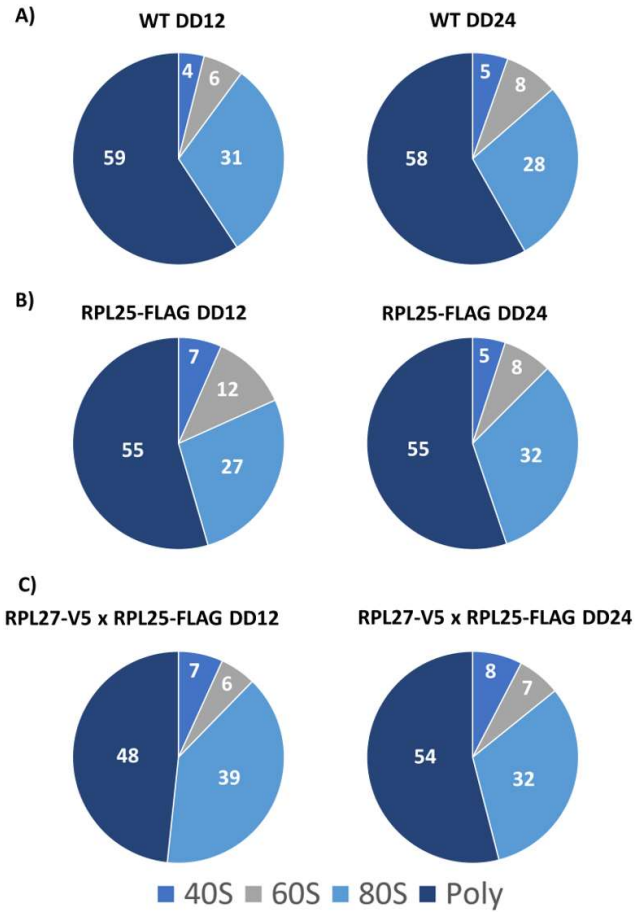

Figure 16. A comparison of sucrose density gradient profiles. Pie charts showing the relative amounts of the 40S and 60S subunits, the 80S monosomes, and polysomes of (A) WT, (B) RPL25-FLAG, and (C) RPL27-V5 x RPL25-FLAG sucrose density gradient profiles at two different time points DD12 and DD24. (A) n=2; B) and (C) n=1.

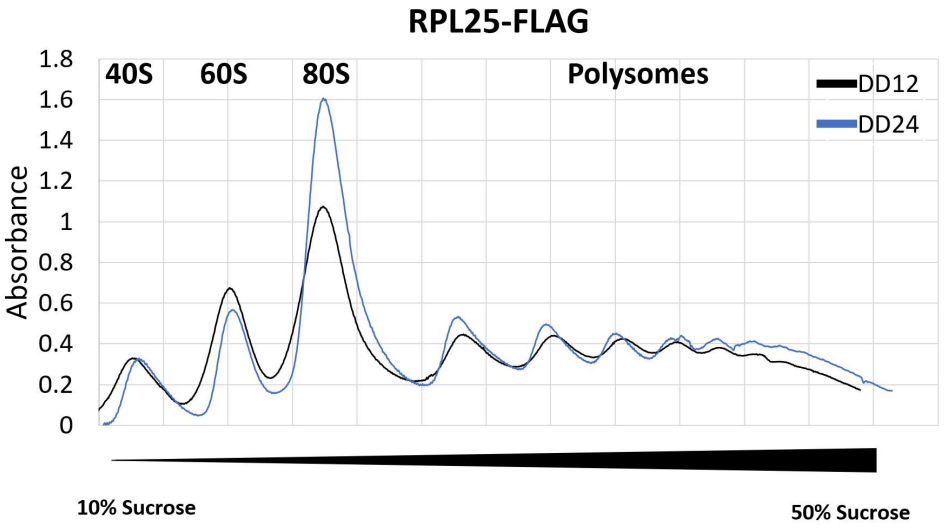

Figure 17. Sucrose density gradient profile of RPL25-FLAG cells at two different time points, DD12 and DD24. Profile was normalized to 0; n=1.

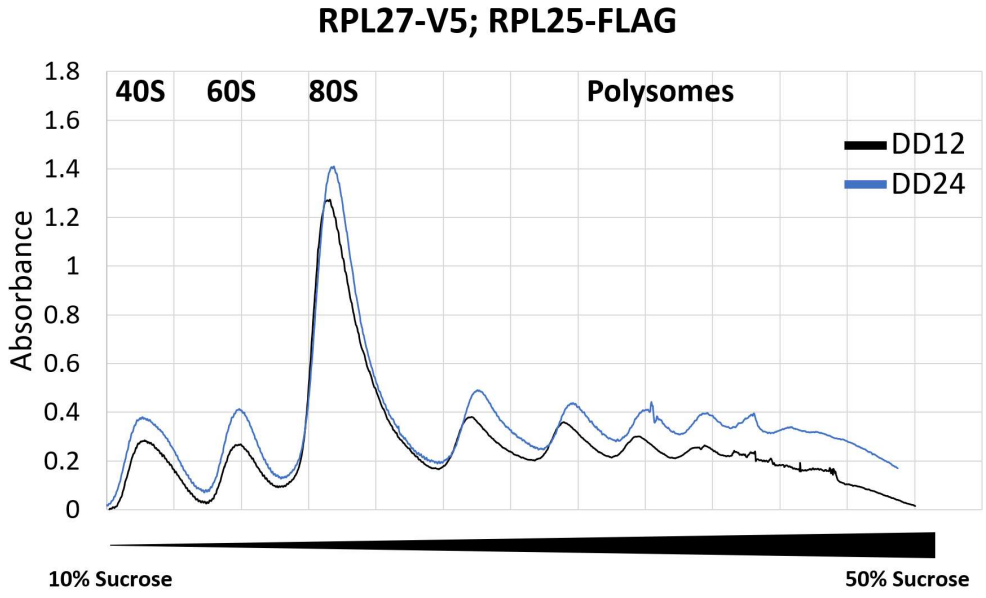

Figure 18. Sucrose density gradient profile of RPL27-V5; RPL25-FLAG cells at two different time points, DD12 and DD24. Profile was normalized to 0; n=1.

4. SUMMARY

4.1 Circadian regulation of differential ribosome composition in pelleted ribosomes

Previous studies have shown that in addition to the role of the circadian clock in rhythmic transcript abundance [22, 30, 42, 46, 49] the clock also influences rhythmicity at the translational and post-translational levels [7, 25, 26, 36, 37]. However, the effect of the circadian clock on differential composition of ribosomes, and in turn, how that effects translation, is unknown. Differential composition of ribosomes has been seen in other eukaryotic organisms, specifically in different developmental states, modifications to the ribosomal proteins, and in accessory proteins associated with the ribosome [22, 33, 49, 50, 55, 62]. In addition, genome-wide studies indicated ribosomes are heterogenous in their core ribosomal protein composition and there are rhythms associated with accumulation of the ribosomal protein mRNAs [55, 56]. Using V5-epitope-tagged ribosomal proteins in *N. crassa*, this study focused on determining if the circadian clock regulates the levels of specific ribosomal proteins in pelleted ribosomes. Furthermore, cell fractionation was employed to examine the possibility of rhythms in polysome and ribosomal subunit abundance as a function of the time-of-day.

Analysis of MS/MS data from TAMU and EMSL led to the prediction that 15 ribosomal proteins in *N. crassa* may vary in abundance in ribosomes throughout the day (Table 1). For this study, I focused on two of the four ribosomal proteins (RPL27 and RPS19) that were predicted to be rhythmic in both data sets, and performed independent experiments to test their rhythmicity.

Using V5-epitope tags, homokaryon strains of the two predicted rhythmic ribosomal proteins (RPL27 and RPS19) were generated (predicted rhythmic RP::6xGLY::V5::*hph*). Homokaryotic RPL27-V5 and RPS19-V5-tagged strains were generated, and they exhibited WT

growth rates when grown on selective media, suggesting that the tagged ribosomal proteins are at least partially functional. Additionally, I was able to generate a dual-tagged strain (RPL27-V5; RPL25-FLAG) and polysomes were identified containing both tags, indicating that the dual-tagged ribosomes are capable of some level of translation to maintain growth.

Pelleted ribosomes of the V5-tagged strains (RPL27-V5 and RPS19-V5) were analyzed through western blot to determine the levels of the specific ribosomal proteins. The expectation was that these ribosomal proteins would cycle throughout the day and have peak times corresponding to the MS/MS protein abundance peak; however, that was not the case. RPL27-V5 (DBP2720) protein abundance was not rhythmic in pelleted ribosomes from cycling cultures (Figure 12). In addition, RPS19-V5 (DBP2754) protein was arrhythmic in pelleted ribosomes in three independent replicates (Figure 13). However, RPS19-V5 shows possible rhythmicity in two of the three replicates, with similar peaks and troughs, suggesting a low amplitude rhythm (Figure 14D). Additionally, the average of two replicates displayed a rhythm very similar to the rhythm observed from the MS/MS normalized peptide reads plot (Figure 14E). A low amplitude rhythm is more difficult to experimentally validate than one with high amplitude, so more replicates are being performed to increase the statistical power of the rhythm tests.

There are a few reasons that could explain the lack of rhythmicity seen in these ribosomal protein samples. First, a hygromycin B cassette interrupts the 3' UTR of these tagged ribosomal proteins, which could potentially interfere with rhythmic regulation of ribosomal protein expression. Second, the V5-tag itself could influence the protein rhythmicity. Finally, the MS/MS data may have shown a larger variation of these ribosomal protein levels throughout the day, which could mislead us into thinking they are rhythmic when they are not.

Overall this method of validating rhythmicity of the ribosomal proteins shows promise, but there are still challenges which need to be overcome. Currently, the ribosomal protein strains are being re-tagged with constructs which no longer contain hygromycin B (RP::6xGLY::V5). These new constructs will ensure that there is no interruption of the 3' UTR. Additionally, available ribosomal protein antibodies are currently being used to detect the levels of the WT proteins.

4.2 Sucrose density gradient profile analysis

Sucrose density gradient fractionation was used to examine the profiles of WT, RPL25-FLAG (DBP2512), and RPL27-V5; RPL25-FLAG (DBP2825) strains to determine possible time-of-day differences, and to examine if the tag may be affecting incorporation of the ribosomal protein into the actively translating ribosome. For these experiments I chose two timepoints, subjective morning and subjective evening (DD12 and DD24) to determine if I could observe a time-of-day difference in a sucrose density gradient profile of an untagged strain. It was predicted in the WT strain, there would be more polysomes at night (DD24) because that is when *N. crassa* is predicted to be translationally active [6, 22]. WT sucrose density gradient profiles (Figure 15), and the percent of different components of the ribosome (monosomes versus polysomes), showed no discernable time-of-day difference (Figure 16) in the individual components of the ribosome. These data indicate that there may be no clear circadian rhythm in translating ribosomes; however, more experiments with additional timepoints need to be performed to confirm these findings.

To determine if the epitope tags have any functional consequences in the actively translating ribosomes, sucrose density gradient fractionation was performed on both RPL25-

FLAG and RPL27-V5; RPL25-FLAG. It was predicted that the profiles should exhibit the same trend and similar amounts of the components of the ribosome (40S, 60S, 80S, and polysomes) if there was no consequence on translation for ribosomes containing tagged ribosomal proteins. However, at DD12, the incorporation of a single and dual-tagged ribosomal proteins altered the ratio of the translating ribosomes (Figure 16). In the tagged profiles, there was a decrease in the number of polysomes in both the single and dual-tagged strain, suggesting the tags interfere with translation. To circumvent this problem, our current plans are to use ribosomal protein antibodies against the endogenous protein, which requires no tagging or inadvertent disruption of the ribosomal proteins. Furthermore, testing additional timepoints and increasing the number of replicates may confirm changes in the ribosomal composition, or uncover time-of-day differences in monosomes verses polysomes.

4.3 Future prospects

Our long-term goal is to determine if the circadian clock controls the composition of the ribosome, and if so, does this affect rhythmic mRNA translation generally or are specific mRNAs regulated. Through using strains without the hygromycin B cassette interruption of the 3' end of the gene, which may contain regulatory elements, or by using antibodies against ribosomal proteins to circumvent having to tag the ribosomal proteins, we expect to determine the rhythmicity of ribosomal proteins present in pelleted ribosomes or polysomes. Once rhythmicity of specific ribosomal proteins present in ribosomes is established, we can determine if the ribosomal proteins have a general effect on translation, meaning the composition of the ribosome widely effects mRNA translation, or if a specific effect on the translation of certain mRNAs or groups of mRNAs occurs. For example, deletion or constitutive expression strains of

rhythmic ribosomal proteins can be used in ribosome profiling experiments, and the effects of translation can be compared to WT and ΔFRQ strains, to determine if rhythms in ribosomal proteins associated with the ribosome influence all or specific mRNA translation.

REFERENCES

1. Baker, C.L., J.J. Loros, and J.C. Dunlap, *The circadian clock of Neurospora crassa.* FEMS Microbiol Rev, 2012. **36**(1): p. 95-110.

2. Beadle, G.W. and E.L. Tatum, *Genetic Control of Biochemical Reactions in Neurospora.* Proceedings of the National Academy of Sciences of the United States of America, 1941. **27**(11): p. 499-506.

3. Bell-Pedersen, D., *Understanding circadian rhythmicity in Neurospora crassa: from behavior to genes and back again.* Fungal Genet Biol, 2000. **29**(1): p. 1-18.

4. Bennett, L.D., et al., *Circadian activation of the mitogen-activated protein kinase MAK-1 facilitates rhythms in clock-controlled genes in Neurospora crassa.* Eukaryot Cell, 2013. **12**(1): p. 59-69.

5. Bobrowicz, P., et al., *The Neurospora crassa pheromone precursor genes are regulated by the mating type locus and the circadian clock.* Molecular Microbiology, 2002. **45**(3): p. 795-804.

6. Brunner, M. and T. Schafmeier, *Transcriptional and post-transcriptional regulation of the circadian clock of cyanobacteria and Neurospora.* Genes & Development, 2006. **20**(9): p. 1061-1074.

7. Caster, S.Z., et al., *Circadian clock regulation of mRNA translation through eukaryotic elongation factor eEF-2.* Proc Natl Acad Sci U S A, 2016. **113**(34): p. 9605-10.

8. Chang, B. and H. Nakashima, *Effects of light-dark cycles on the circadian conidiation rhythm in Neurospora crassa.* Journal of Plant Research, 1997. **110**(4): p. 449-453.

9. Cheng, P., et al., *Coiled-coil domain-mediated FRQ-FRQ interaction is essential for its circadian clock function in Neurospora.* EMBO J, 2001. **20**(1-2): p. 101-8.

10. Cheng, P., Y. Yang, and Y. Liu, *Interlocked feedback loops contribute to the robustness of the Neurospora circadian clock.* Proc Natl Acad Sci U S A, 2001. **98**(13): p. 7408-13.

11. Colon-Ramos, D.A., et al., *Direct ribosomal binding by a cellular inhibitor of translation.* Nat Struct Mol Biol, 2006. **13**(2): p. 103-11.

12. Correa, A., et al., *Multiple oscillators regulate circadian gene expression in Neurospora.* Proc Natl Acad Sci U S A, 2003. **100**(23): p. 13597-602.

13. Davis, R.H., *Neurospora: Contributions of a Model Organism*. 2000, New York: Oxford University Press.

14. Davis, R.H. and F.J. de Serres, *[4] Genetic and microbiological research techniques for Neurospora crassa*, in *Methods in Enzymology*. 1970, Academic Press. p. 79-143.

15. Dekhang, R., et al., *The Neurospora Transcription Factor ADV-1 Transduces Light Signals and Temporal Information to Control Rhythmic Expression of Genes Involved in Cell Fusion.* G3 (Bethesda), 2017. **7**(1): p. 129-142.

16. Dunlap, J.C. and J.J. Loros, *The Neurospora circadian system.* J Biol Rhythms, 2004. **19**(5): p. 414-24.

17. Feldman, J.F. and M.N. Hoyle, *Isolation of Circadian Clock Mutants of NEUROSPORA CRASSA.* Genetics, 1973. **75**(4): p. 605-613.

18. Filipovska, A. and O. Rackham, *Specialization from synthesis: how ribosome diversity can customize protein function.* FEBS Lett, 2013. **587**(8): p. 1189-97.

19. Froehlich, A.C., et al., *White Collar-1, a circadian blue light photoreceptor, binding to the frequency promoter.* Science, 2002. **297**(5582): p. 815-9.

20. Garceau, N.Y., et al., *Alternative initiation of translation and time-specific phosphorylation yield multiple forms of the essential clock protein FREQUENCY.* Cell, 1997. **89**(3): p. 469-76.

21. Goldsmith, C.S., et al., *Inhibition of p38 MAPK activity leads to cell type-specific effects on the molecular circadian clock and time-dependent reduction of glioma cell invasiveness.* BMC Cancer, 2018. **18**(1): p. 43.

22. Hurley, J.M., et al., *Analysis of clock-regulated genes in Neurospora reveals widespread posttranscriptional control of metabolic potential.* Proceedings of the National Academy of Sciences, 2014. **111**(48): p. 16995-17002.

23. Ingolia, N.T., et al., *The ribosome profiling strategy for monitoring translation in vivo by deep sequencing of ribosome-protected mRNA fragments.* Nature Protocols, 2012. **7**: p. 1534.

24. Ingolia, Nicholas T., Liana F. Lareau, and Jonathan S. Weissman, *Ribosome Profiling of Mouse Embryonic Stem Cells Reveals the Complexity and Dynamics of Mammalian Proteomes.* Cell, 2011. **147**(4): p. 789-802.

25. Jang, C., et al., *Ribosome profiling reveals an important role for translational control in circadian gene expression.* Genome Res, 2015. **25**(12): p. 1836-47.

26. Janich, P., et al., *Ribosome profiling reveals the rhythmic liver translatome and circadian clock regulation by upstream open reading frames.* Genome Res, 2015. **25**(12): p. 1848-59.

27. Jouffe, C., et al., *The Circadian Clock Coordinates Ribosome Biogenesis.* PLOS Biology, 2013. **11**(1): p. e1001455.

28. Karatsoreos, I.N., *Links between Circadian Rhythms and Psychiatric Disease.* Frontiers in Behavioral Neuroscience, 2014. **8**: p. 162.

29. Ko, C.H. and J.S. Takahashi, *Molecular components of the mammalian circadian clock.* Human Molecular Genetics, 2006. **15**(suppl_2): p. R271-R277.

30. Koike, N., et al., *Transcriptional Architecture and Chromatin Landscape of the Core Circadian Clock in Mammals.* Science (New York, N.Y.), 2012. **338**(6105): p. 349-354.

31. Kojima, S., D.L. Shingle, and C.B. Green, *Post-transcriptional control of circadian rhythms.* J Cell Sci, 2011. **124**(Pt 3): p. 311-20.

32. Kondo, T., et al., *Circadian clock mutants of cyanobacteria.* Science, 1994. **266**(5188): p. 1233-6.

33. Kondrashov, N., et al., *Ribosome mediated specificity in Hox mRNA translation and vertebrate tissue patterning.* Cell, 2011. **145**(3): p. 383-397.

34. Lamb, T.M., J. Vickery, and D. Bell-Pedersen, *Regulation of Gene Expression in Neurospora crassa with a Copper Responsive Promoter.* G3: Genes|Genomes|Genetics, 2013. **3**(12): p. 2273-2280.

35. Lee, K., J.C. Dunlap, and J.J. Loros, *Roles for WHITE COLLAR-1 in circadian and general photoperception in Neurospora crassa.* Genetics, 2003. **163**(1): p. 103-14.

36. Lidder, P., et al., *Circadian control of messenger RNA stability. Association with a sequence-specific messenger RNA decay pathway.* Plant Physiol, 2005. **138**(4): p. 2374-85.

37. Lim, C. and R. Allada, *Emerging roles for post-transcriptional regulation in circadian clocks.* Nat Neurosci, 2013. **16**(11): p. 1544-50.

38. Liu, Y. and D. Bell-Pedersen, *Circadian rhythms in Neurospora crassa and other filamentous fungi.* Eukaryot Cell, 2006. **5**(8): p. 1184-93.

39. Liu, Y., J. Loros, and J.C. Dunlap, *Phosphorylation of the Neurospora clock protein FREQUENCY determines its degradation rate and strongly influences the period length of the circadian clock.* Proc Natl Acad Sci U S A, 2000. **97**(1): p. 234-9.

40. Luo, Z., M. Freitag, and M.S. Sachs, *Translational regulation in response to changes in amino acid availability in Neurospora crassa.* Mol Cell Biol, 1995. **15**(10): p. 5235-45.

41. Margolin, B.S., M. Freitag, and E.U. Selker, *Improved plasmids for gene targeting at the his-3 locus of Neurospora crassa by electroporation.* Fungal Genetics Report, 1997. **44**(1): p. 34-36.

42. Menet, J.S., et al., *Nascent-Seq reveals novel features of mouse circadian transcriptional regulation.* eLife, 2012. **1**: p. e00011.

43. Michael, J.M. and K.W. David, *Cellular Circadian Clocks in Mood Disorders.* Journal of Biological Rhythms, 2012. **27**(5): p. 339-352.

44. Montenegro-Montero, A. and L. Larrondo, *The Neurospora Circadian System: From Genes to Proteins and Back, in Less Than 24 Hours*, in *Neurospora: Genomics and Molecular Biology*. 2013, Caister Academic Press: UK.

45. Panda, S., J.B. Hogenesch, and S.A. Kay, *Circadian rhythms from flies to human.* Nature, 2002. **417**(6886): p. 329-35.

46. Partch, C.L., C.B. Green, and J.S. Takahashi, *Molecular Architecture of the Mammalian Circadian Clock.* Trends in cell biology, 2014. **24**(2): p. 90-99.

47. Pasa-Tolic, L., et al., *Proteomic analyses using an accurate mass and time tag strategy.* Biotechniques, 2004. **37**(4): p. 621-4, 626-33, 636 passim.

48. Pittendrigh, C.S., et al., *Growth Patterns in Neurospora: A Biological Clock in Neurospora.* Nature, 1959. **184**: p. 169.

49. Ramagopal, S., *Induction of cell-specific ribosomal proteins in aggregation-competent nonmorphogenetic Dictyostelium discoideum.* Biochem Cell Biol, 1990. **68**(11): p. 1281-7.

50. Ramagopal, S. and H.L. Ennis, *Regulation of synthesis of cell-specific ribosomal proteins during differentiation of Dictyostelium discoideum.* Proc Natl Acad Sci U S A, 1981. **78**(5): p. 3083-7.

51. Reddy, A.B., et al., *Circadian orchestration of the hepatic proteome.* Curr Biol, 2006. **16**(11): p. 1107-15.

52. Rivera, M.C., B. Maguire, and J.A. Lake, *Isolation of ribosomes and polysomes.* Cold Spring Harb Protoc, 2015. **2015**(3): p. 293-9.

53. Sauert, M., H. Temmel, and I. Moll, *Heterogeneity of the translational machinery: Variations on a common theme.* Biochimie, 2015. **114**: p. 39-47.

54. Schafmeier, T., et al., *Transcriptional feedback of Neurospora circadian clock gene by phosphorylation-dependent inactivation of its transcription factor.* Cell, 2005. **122**(2): p. 235-46.

55. Shi, Z., et al., *Heterogeneous Ribosomes Preferentially Translate Distinct Subpools of mRNAs Genome-wide.* Mol Cell, 2017. **67**(1): p. 71-83.e7.

56. Simsek, D., et al., *The Mammalian Ribo-interactome Reveals Ribosome Functional Diversity and Heterogeneity.* Cell. **169**(6): p. 1051-1065.e18.

57. Smith, K.M., et al., *Transcription factors in light and circadian clock signaling networks revealed by genomewide mapping of direct targets for neurospora white collar complex.* Eukaryot Cell, 2010. **9**(10): p. 1549-56.

58. Turek, F.W., et al., *Obesity and metabolic syndrome in circadian Clock mutant mice.* Science, 2005. **308**(5724): p. 1043-5.

59. Vitalini, M.W., et al., *The rhythms of life: circadian output pathways in Neurospora.* J Biol Rhythms, 2006. **21**(6): p. 432-44.

60. White, K., et al., *Genetic control of programmed cell death in Drosophila.* Science, 1994. **264**(5159): p. 677-683.

61. Wu, G., et al., *MetaCycle: an integrated R package to evaluate periodicity in large scale data.* Bioinformatics, 2016. **32**(21): p. 3351-3353.

62. Xue, S. and M. Barna, *Specialized ribosomes: a new frontier in gene regulation and organismal biology.* Nat Rev Mol Cell Biol, 2012. **13**(6): p. 355-69.

63. Zimmer, J.S., et al., *Advances in proteomics data analysis and display using an accurate mass and time tag approach.* Mass Spectrom Rev, 2006. **25**(3): p. 450-82.